Biochemical and Biophysical Research Communications **288,** 121–128 (2001)
doi:10.1006/bbrc.2001.5732, available online at http://www.idealibrary.com on IDEAL®

Characterization of Thermal Stability of the *Escherichia coli* Fapy–DNA Glycosylase

Serguei V. Kuznetsov,*[,1] Olga M. Sidorkina,† Jacques Laval,† and Anjum Ansari*[,‡,1]
**Department of Physics (MC 273) and ‡Department of Bioengineering (MC 063), University of Illinois at Chicago, 845 West Taylor Street, Chicago, Illinois 60607; and †Groupe "Réparation de l'ADN," UMR 8532, CNRS, Institut Gustave Roussy, 39, rue Camille Desmoulins, 94805 Villejuif Cedex, France*

Received September 14, 2001

Thermal stability of *Escherichia coli* Fpg protein was studied using far-UV circular dichroism and intrinsic fluorescence. Experimental data indicate that Fpg irreversibly aggregates under heating above 35°C. Heat aggregation is preceded by tertiary conformational changes of Fpg. However, the secondary structure of the fraction that does not aggregate remains unchanged up to ~60°C. The kinetics of heat aggregation occurs with an activation enthalpy of ~21 kcal/mol. The fraction of monomers forming aggregates decreases with increasing urea concentration, with essentially no aggregation observed above ~3 M urea, suggesting that heat aggregation results from hydrophobic association of partially unfolded proteins. With increasing urea concentration, Fpg unfolds in a two-state reversible transition, with a stability of ~3.6 kcal/mol at 25°C. An excellent correlation is observed between the unfolded fraction and loss of activity of Fpg. A simple kinetic scheme that describes both the rates and the extent of aggregation at each temperature is presented.

Key Words: **DNA repair enzyme; formamidopyrimidine–DNA glycosylase; thermal stability; heat aggregation; kinetics of aggregation.**

In cells, DNA is continuously being damaged by highly reactive oxygen species formed as a result of ionizing radiation, chemicals, and as a consequence of metabolism (1, 2). One of the most stable products of oxidative DNA damage is the 8-oxoguanine lesion. If not repaired, oxidative DNA lesions can lead to deleterious cellular consequences such as aging, a number of diseases including cancer, and cell death (3). A number of repair pathways catalyzed by DNA repair enzymes exist to prevent this kind of DNA damage. One such DNA repair enzyme identified in *Escherichia coli* is the Fpg protein (2,6-diamino-4-hydroxy-5*N*-methylformamidopyrimidine [Fapy]–DNA glycosylase) (4).

The Fpg protein from *E. coli* is a globular monomer of 30.2 kDa with 269 amino acid residues and contains one zinc atom in a zinc finger motif. Its active site is located within the first 73 residues from the amino terminus (5). *In vivo* Fpg, together with MutY protein, is involved in the removal of oxidatively damaged form of 7,8-dihydro-8-oxoguanine residues in DNA (6). *In vitro* Fpg excises a broad spectrum of modified purines (1, 7). It has an apurinic/apyrimidinic (AP) lyase activity that incises DNA at abasic sites by a β-δ elimination mechanism (8, 9), and excises 5′-terminal deoxyribose phosphate from pre-incised AP site (10).

Studies of the structure–function relation of Fpg, and an understanding of the lesion recognition at the atomic level, have been hampered by the lack of detailed structural information because of the difficulty in crystallizing the Fpg protein from *E. coli*. Recently, Kuramitsu and co-workers have been successful in crystallizing the corresponding protein, MutM (Fpg), from an extremely thermophilic bacterium, *Thermus thermophilus* HB8 (11). Characterization of the stability of *T. thermophilus* MutM protein showed that the protein is stable against heat, pH and chemical denaturation, and retains 8-oxoguanine DNA glycosylase activity up to at least 60°C. In contrast, the *E. coli* Fpg protein was found to be less stable and active only up to ~37°C (12).

The instability of *E. coli* Fpg and the unsuccessful attempts by several groups to crystallize the protein has prompted a detailed investigation of its thermal stability. In a recent study, where the thermal unfolding of the *E. coli* Fpg was monitored using circular dichroism (CD) techniques, the ellipticity at 220 nm was found to decrease sharply and irreversibly above ~55°C (13). The authors of that study interpreted their result as two-state unfolding of the protein. Here, we present evidence that the irreversible drop in the CD

[1] To whom correspondence may be addressed at Department of Physics (MC 273), University of Illinois at Chicago, 845 West Taylor Street, Chicago, IL 60607. Fax: 312-996-9016. E-mail: ansari@uic.edu or skouznet@uic.edu.

0006-291X/01 $35.00

signal with increasing temperature is a consequence of aggregation of the Fpg protein and that only the fraction of proteins that has not aggregated contributes to the CD signal at each temperature. We find that heat aggregation starts at physiological temperatures (~30–35°C), and is preceded by partial denaturation of Fpg. The secondary structure of the fraction that remains monomeric is stable up to at least 60°C. Heat aggregation is inhibited both by addition of glycerol as well as by an increase in urea concentration, which reduces hydrophobic association of the partially denatured conformers. Urea denaturation, monitored using spectral shifts in the intrinsic Trp fluorescence, is found to exhibit a classic two-state folding/unfolding transition, which is completely reversible. The fact that Trp fluorescence shifts accurately monitor the fraction of unfolded proteins is confirmed by the excellent correlation observed between the spectral shifts in Trp fluorescence and the measured loss of activity. Finally, we have measured the kinetics of heat aggregation as a function of temperature and urea concentration. A simple kinetic scheme that describes both the rates and the extent of aggregation at each temperature is presented.

MATERIALS AND METHODS

Purification of the Fpg protein. Fpg was purified from *E. coli* BH20 containing the $pFPG_{220}$ plasmid. The procedure for the overproduction and purification of the *fpg* gene product was essentially as described by Boiteux *et al.* (14). Fpg was identified by its molecular mass and its purity was determined using 12% SDS–PAGE. Then, the enzyme was dialyzed in 20 mM Hepes, pH 7.8, 1 mM EDTA, 300 mM NaCl, 1 mM DTE and 50% (wt/wt) glycerol at 4°C and stored at −20°C. Before CD and fluorescence measurements, fresh samples were prepared by dialyzing the stock solution of the Fpg against 20 mM sodium phosphate buffer, pH 7.4.

Fapy-DNA glycosylase assay in the presence of urea. 19 samples of the Fpg and 19 samples of [^{3}H]Fapy-poly(dG-dG) were prepared in 20 mM $NaPO_4$, pH 7.4, 100 mM NaCl, 1 mM EDTA buffer containing varying concentrations of urea. The samples were incubated overnight. Before measurement solution of [^{3}H]Fapy-poly(dG-dG) was added into each of the corresponding Fpg samples to give final concentration of 5500 cpm of [^{3}H]Fapy-poly(dG-dG) (3900 cpm/pmol of nucleotide) and 30 ng of enzyme in total volume of 50 μl, and final urea concentration ranging from 0 to 6 M. After incubation of the samples for 10 min at 37°C, the ethanol-soluble [^{3}H]Fapy residues were separated and quantified as described (14). One enzyme unit is defined as the amount of the Fpg that releases 1 pmol of [^{3}H]Fapy during 10 min at 37°C under the assay conditions. As a control, the Fpg with 0 M urea was used.

Circular dichroism and fluorescence measurements. Far-UV CD spectra were measured with a JASCO J-600 (Easton, MD) spectropolarimeter over the range of 186–260 nm using a strain-free quartz cuvette of path length 0.1 cm. The spectra were obtained as the average of eight scans and were corrected with a baseline obtained for the solvent in the same experimental conditions and the same cell. The temperature of the sample was maintained with a RTE 111 Neslab bath system, and monitored by a thermocouple in direct contact with the cuvette.

Fluorescence and scattered light measurements were carried out with a FluoroMax-2 (Jobin Yvon-Spex, Edison, NJ) spectrofluorometer. Cylindrical quartz cuvettes of 250 μl were used. An excitation wavelength of 295 nm was used to preferentially excite the five tryptophan residues and to minimize excitation of eight tyrosine residues present in the Fpg (14). Emission spectra as a function of temperature and urea were collected from 305 to 450. For the aggregations kinetics, fluorescence intensity at 340 nm was measured as a function of time. Scattered light from the sample was monitored at 450 nm with excitation at the same wavelength.

Equilibrium urea denaturation. Stock urea solutions at concentration 0.5–8 M were prepared gravimetrically. The samples, after addition of urea, were stored overnight at 4°C and then used. The fluorescence intensity of the Fpg protein are found to be insensitive to urea concentration between 0 and 8 M. Therefore, the fluorescence spectral shift as a function of urea was used to monitor the denaturation of Fpg. The denaturation curves were analyzed in terms of a two-state system. We used the linear extrapolation model for describing denaturant-induced unfolding $\Delta G_{un} = \Delta G^0_{un} - m[\mathrm{d}]$ (15). Here ΔG_{un} is the free energy change for unfolding of proteins in the presence of denaturant, ΔG^0_{un} is the free energy change in the limit of no denaturant, m is a denaturant susceptibility parameter and [d] is the concentration of denaturant. The apparent value of ΔG^0_{un} (protein stability) can be calculated as $\Delta G^0_{un} = m[\mathrm{d}]_{1/2}$, where $[\mathrm{d}]_{1/2}$ is the concentration of the denaturant at which half the proteins are denatured.

The experimental points were fitted to the following equation

$$F = \frac{F_N + F_D \exp[-\Delta G_{un}/RT]}{1 + \exp[-\Delta G_{un}/RT]}. \quad [1]$$

Here F is the amplitude of the spectral shift at the given denaturant concentration, R is the gas constant, and T is the temperature in Kelvin. F_N and F_D are the baselines at low (N) and high (D) denaturant concentrations, respectively. The best fit values of m and $[\mathrm{d}]_{1/2}$ and their standard errors were obtained from nonlinear least-squares analysis.

Kinetics of aggregation. The sample was first equilibrated at T_{ref} = 25°C and then placed into the sample holder of the fluorescence spectrofluorometer equilibrated at temperature T. The characteristic time constant (τ_{eq}) for the temperature of the sample to reach the final temperature T of the sample holder was measured by monitoring the temperature inside a cuvette containing only the buffer. The temperature of the sample was measured by placing a YSI 44008 Precision Thermistor in direct contact with the cuvette. In our experimental setup, $\tau_{eq} = 61 \pm 0.4$ s. For the Fpg sample, an initial drop in the fluorescence of the sample is observed during temperature equilibration as a result of a change in the quantum yield of Trp as a function of temperature. This change is given by $I(t, T) = \Delta I^{eq}_F(T)\exp(-t/\tau_{eq})$ where $\Delta I^{eq}_F(T)$ is the amplitude of the decrease in the quantum yield of Trp from T_{ref} to T. ΔI^{eq}_F was determined from the temperature-dependence of the fluorescence intensity of Fpg in the presence of 50% w/w glycerol (Fig. 2). Under these solvent conditions there is no heat aggregation up to ~60°C and the change in fluorescence intensity as a function of temperature arises primarily from a change in the quantum yield. The relative change of the fluorescence intensity of the Fpg sample from a 1 K change of temperature is $(0.0099 \pm 0.005)\ \mathrm{K}^{-1}$. This value is very close to the value of ~0.01 observed for free tryptophan. The fluorescence intensity corrected for the temperature-dependent change in the quantum yield was obtained at each final temperature T by subtracting the initial drop $I(t, T)$ from the measured intensity.

RESULTS

Effect of temperature on far-UV CD and fluorescence spectra of Fpg. Far-UV CD spectra of Fpg protein exhibit one negative peak at 207 nm with a shoulder at

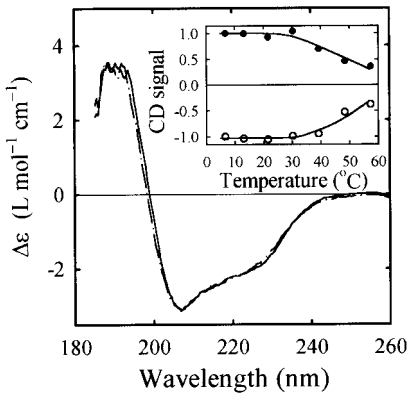

FIG. 1. Far-UV CD spectra of Fpg at 20°C (—) and 57.5°C (— · —). Spectrum at 57.5°C was multiplied by a factor of 2.94 in order to match the 20°C spectrum at 207 nm. (Inset) Amplitudes of the CD signal at 190 nm (—●—) and 222 nm (—○—) versus temperature. The spectra were collected in the direction of low to high temperatures. The amplitudes measured at the lowest temperature (6°C) were normalized to +1 at 190 nm and −1 at 222 nm.

222 nm indicating that the protein has a largely structured conformation. The spectral shapes monitored between 20 and ~58°C are identical to within a multiplicative factor (Fig. 1), but the amplitude of the CD signal decreases irreversibly with increasing temperature above ~30–35°C (Fig. 1, inset).

The fluorescence intensity decreases reversibly with increasing temperature up to ~35°C (Fig. 2) as a result of a change in the quantum yield of Trp. Above ~35°C the decrease in intensity is irreversible. This decrease is accompanied by a shift in the fluorescence spectra to longer wavelengths with essentially no change in the spectral shape (Fig. 2, inset). The total spectral shift

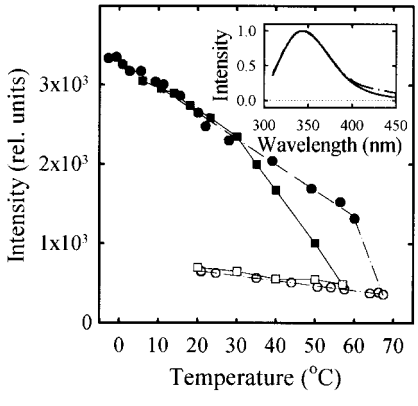

FIG. 2. Fluorescence intensity of Fpg versus temperature. Filled symbols correspond to fluorescence measurements in the direction of increasing temperature and open symbols correspond to fluorescence measurements in the direction of decreasing temperature. —■—, solvent is identical to the one used for the CD measurements; —●— · —, solvent with 50% w/w glycerol. (Inset) The fluorescence spectra of Fpg recorded at 20°C (—) and 60°C (— · —). Spectrum at 60°C was multiplied by a factor of 2.84 and shifted by 3 nm to the blue to maximize the overlap with the spectrum at 20°C.

between 5 and 60°C is ~3 nm. A slight increase in the intensity at the longer wavelengths of the fluorescence spectrum acquired at 60°C is a result of an increase in the scattered light from the sample, indicating an increasing amount of aggregated proteins at higher temperatures. In the presence of 50% w/w glycerol the decrease in the fluorescence amplitude as a function of temperature becomes irreversible only at temperatures above ~60°C (Fig. 2).

The effect of temperature on the conformation of Fpg is summarized in Fig. 3. The change in the amplitude of the CD signal, normalized between 0 and 1, is plotted with the spectral shifts of the Trp fluorescence spectra. Both signals indicate a change between 30 and 40°C, accompanied by a loss of transparency of the sample, suggesting the onset of heat aggregation. A direct measure of aggregation is the increase in scattered light at 450 nm, and is plotted in Fig. 3 for comparison. The difference of about 5–10°C observed in the onset of heat aggregation as measured by the different probes reflects the insensitivity of the spectrometers to measure small changes in the early stages of aggregation. In the presence of 50% w/w glycerol, known to stabilize protein structure (16), the onset of the fluorescence spectral shifts occurs at ~55°C, approximately 15°C higher than the onset observed in the absence of glycerol (Fig. 3).

Kinetics of aggregation. The Trp fluorescence intensity decreases irreversibly above ~30°C, as shown in Fig. 2, and is interpreted as arising from aggregation of the protein. The rate of aggregation decreases with decreasing Fpg concentration (data not shown). All kinetics measurements presented here were done with a concentration of ~10 μM. The kinetics of aggregation were measured for temperatures ranging from 5 to 70°C. The initial drop in intensity, arising from a change in the temperature of the sample prior to equilibrium, was subtracted as described under Materials and Methods. Figure 4 shows two kinetics curves, at 20

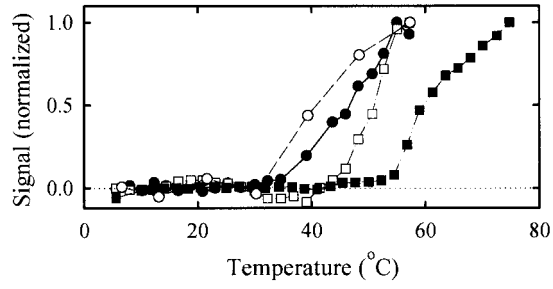

FIG. 3. Temperature dependence of the CD and fluorescence spectra. All the signals are normalized between zero and one to facilitate a comparison. —○—, the change in the amplitude of the CD spectra; —●—; the intensity of the scattered light at 450 nm; —□—, the shift in the fluorescence spectra in the absence of glycerol in the solvent; —■—, the shift in the fluorescence spectra in the presence of 50% w/w glycerol.

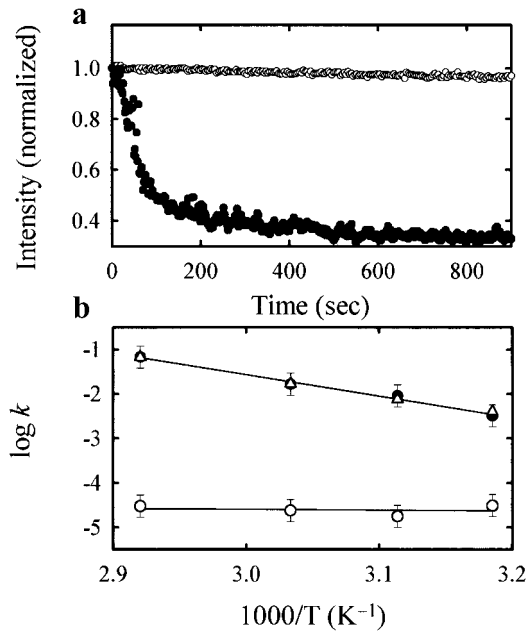

FIG. 4. (a) Kinetics of aggregation as a function of time as monitored by an irreversible decrease in the fluorescence intensity of Fpg at $T = 20°C$ (○) and 56.5°C (●). Excitation wavelength of 295 nm and emission at 340 nm were used. (b) Arrhenius temperature dependence of the relaxation rates obtained from a biexponential fit to the aggregation kinetics. (●) relaxation rate corresponding to the fast (heat aggregation) component; (○) relaxation rate corresponding to the slow (photoinduced aggregation) component; (△) the values of k_{obs} calculated using Eq. [5].

and 56.5°C. Between 5 and 30°C, the decrease in intensity can be described as a single-exponential with a characteristic relaxation rate of $\sim 3 \times 10^{-5}$ s^{-1}. This decrease is a result of photoinduced damage. In an earlier paper, we described UVB-induced damage of Fpg protein at room temperature in the absence of glycerol and urea and showed that the kinetics were single-exponential (17). Indeed, the photoinduced damage is accompanied by photoionization of Trp residue(s) with formation of nonfluorescent products of Trp. Above 35°C, in the absence of glycerol, the kinetics are biexponential. The slow component is still from the photoinduced damage. In fact, under all conditions of solvent and temperature, a component corresponding to photoinduced damage is observed with the same relaxation rate of $\sim 3 \times 10^{-5}$ s^{-1} in our experimental conditions (Fig. 4b).

The fast component, on the other hand, exhibits a strong Arrhenius temperature-dependence with a characteristic rate constant of 3.2×10^{-3} s^{-1} at 40°C and an apparent activation energy $E_a \sim 21$ kcal/mol. The residual amplitude at the end of the fast process is compared with the amplitude of the CD spectra as a function of temperature (Fig. 5). The excellent correlation between the two measurements, together with the loss of transparency of the sample, are a strong indication that the loss in fluorescence in the fast phase and the loss of the CD signal are a result of heat aggregation of the protein. These results suggest that the aggregated protein does not contribute significantly to the observed CD and fluorescence signals. Recall that the shape of the CD signal does not change in the entire temperature range of these measurements, which shows that the secondary structure of the fraction that does not aggregate is unchanged. In the presence of 50% w/w glycerol, the kinetics are single-exponential up to ~60°C with the same relaxation rate as for the slow kinetics observed in the absence of glycerol (data not shown), suggesting that heat aggregation is inhibited in the presence of glycerol.

Urea denaturation measurements. The effect of urea on the thermodynamic stability of Fpg was measured by monitoring the Trp fluorescence emission spectra at various concentrations of urea. A complete emission spectrum was recorded three times and then averaged at each concentration of urea at 25°C. The fluorescence intensity was essentially the same for all urea concentrations. However, a spectral shift of about 13 nm from 0 to 6 M urea was observed. The urea dependence of the spectral shift is described very well by a two-state cooperative transition with $[d]_{1/2} = 2.98 \pm 0.02$ M and $m = 1.20 \pm 0.04$ kcal/mol per 1 mol (Fig. 6), yielding a value of $\Delta G^0_{un} = 3.6$ kcal/mol. Figure 6 also shows an excellent correlation between the unfolded fraction of Fpg, obtained from the spectral shift denaturation curve, and its loss of activity with increasing urea concentration. This result shows that the shift in Trp fluorescence as a function of urea concentration is indeed a reliable monitor of the fraction of denatured molecules.

Effect of urea on the kinetics of aggregation. The kinetics of irreversible change of the fluorescence in the presence of denaturant were measured at 40°C for urea concentrations ranging from 0 to 6 M. The kinetics are biexponential at low concentrations of urea; the fast

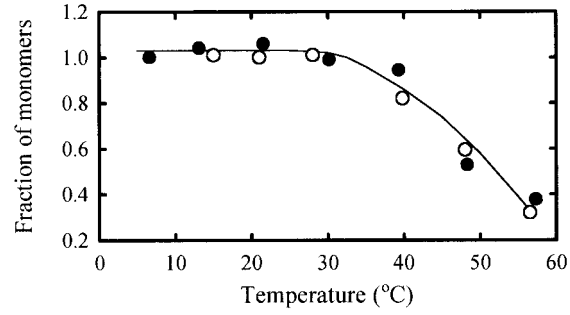

FIG. 5. Fraction of Fpg molecules that do not aggregate during the heat aggregation process. (●) Normalized amplitude of the CD spectra as a function of temperature; (○) the residual fluorescence amplitude $[M]_\infty/[M]_0$ obtained from the fraction of monomers that remain at the end of the fast (heat aggregation) process. The continuous line is drawn to guide the eye.

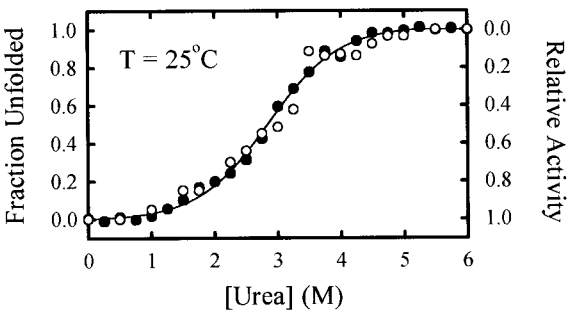

FIG. 6. Fraction unfolded (●) and relative activity (○) of Fpg as a function of urea concentration at $T = 25°C$. The continuous line is obtained from Eq. [1] after subtracting the baselines.

component corresponds to heat aggregation and the slow component corresponds to photoinduced damage (Fig. 7). At high concentrations of urea (above ~3 M) only a single exponential is observed with essentially the same relaxation rate as the slow component under 0 M urea. Note that at 3 M urea, where half the molecules are still in the active state, the heat aggregation is negligible.

DISCUSSION

Heat aggregation of Fpg. The temperature dependence of the far-UV CD signal of Fpg shows an irreversible decrease in the amplitude of the CD signal above ~30–35°C (Fig. 1: inset). The correlation between the decrease of the CD signal and an increase in the scattered light with increasing temperature (Fig. 3) is a strong indication that the irreversible decrease of CD signal comes from the loss of transparency of the sample as a result of heat aggregation of Fpg. This conclusion is further corroborated by the excellent correlation observed between the loss in CD signal and the loss in the amplitude of Trp fluorescence in the fast phase of the observed kinetics (Fig. 5). The shape of the CD spectrum remains unchanged (Fig. 1) indicating that the secondary structure of the fraction of Fpg that remains as monomers at each temperature is not disturbed from 5 to 60°C. It should be noted that there is no significant aggregation during acquisition of spectra. The spectra were recorded after equilibrating the sample at each temperature for ~10 min, while the time constant for the fast phase of aggregation varies from ~5 min to ~15 s in the range of temperatures between 40 and 70°C (Fig. 4). The time constant for the slow phase of aggregation is ~9 h, which is much longer than the time for each spectral acquisition (~8 min).

We have analyzed the CD spectrum of Fpg using the CONTIN procedure as described under Materials and Methods (18). The analysis indicates that 25% of amino acids are in α-helical form, and 31% contribute to the β-sheets. The value of 25% for α-helices is very close to the value of 24.6% obtained for the MutM, Fpg protein from *T. thermophilus* HB8 whose X-ray structure has recently been determined (11). However, the value of 31% for β-sheets is 1.4 times larger than that for the Fpg protein from *T. thermophilus* HB8. Because of the high propensity of β-sheets to aggregate, it is possible that the lower β-sheet content and higher structural stability of the Fpg protein from *T. thermophilus* HB8 makes this protein more resistant to aggregation than the Fpg protein from *E. coli*. It is important to note that even for the Fpg protein from *T. thermophilus* HB8, the CD signal shows an irreversible decrease above ~75°C (12) suggesting that aggregation may occur for this protein as well, albeit at much higher temperatures.

The Trp fluorescence spectra show a detectable spectral shift at temperatures where aggregation occurs, indicating that the monomers that contribute to the fluorescence spectra undergo a tertiary conformational change. The Trp spectral red shifts show that the tertiary conformational changes are most likely a decrease in the compactness of the native state, resulting in an increased exposure of Trp residues to the solvent. From Fig. 3, it can be seen that the Trp fluorescence spectral shift starts at nearly the same temperature at which the decrease in the CD signal intensity and increase in scattered light occurs. Addition of 50% w/w glycerol increases the temperature for the onset of aggregation to ~60°C (Fig. 2) with a corresponding increase in the temperature at which the Trp fluorescence spectral shifts occur to ~55°C (Fig. 3). From these results we conclude that aggregation occurs as a result of denaturation that leads to the formation of partially unfolded protein conformers with a higher propensity to aggregate. The fact that we do not detect any changes in the shape of the CD spectra as a function of temperature (Fig. 1) indicates that residual native or partially denatured monomers that do not aggregate have their secondary structure intact. Protein denaturation of course implies an ensemble of denatured conformations. However, we cannot probe the extent of denaturation of the monomers that ag-

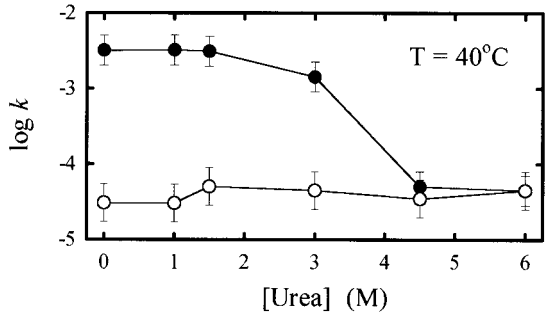

FIG. 7. Characteristic relaxation rates obtained from a biexponential fit to the aggregation kinetics as a function of urea concentration. (●) relaxation rate for the fast component and (○) for the slow component. The kinetics were measured at $T = 40°C$.

gregate, since the steady-state concentration of that fraction is very low, and our CD and fluorescence measurements monitor only the monomers.

Our results are in apparent contradiction with the conclusions drawn by Buchko *et al.* (13) from their thermal denaturation studies on Fpg where they monitor the change in ellipticity at 220 nm as a function of temperature. Buchko *et al.* also observe a sharp drop in ellipticity, although at much higher temperatures, above ~55°C. They interpret the drop in ellipticity as arising from an irreversible unfolding of the protein, leading to a loss in the secondary structure. Our experiments show that the decrease in CD signal with increasing temperature is accompanied by essentially no change in the shape of the CD spectrum, suggesting that we are not monitoring a simple unfolding transition. Since Buchko *et al.* do not present the entire CD spectrum at each temperature, it is difficult to compare our results directly with theirs. However, under identical conditions of solvent, temperature, and protein concentration, their data indicate a puzzling inconsistency; they show that the measured ellipticity at 25°C obtained from a temperature scan at a single wavelength is almost a factor of ×2 larger than the measured ellipticity at 25°C when the entire far-UV CD spectrum is acquired at a single temperature. A likely explanation for this inconsistency is that in the first measurement, the temperature scan is on the same time-scale as the aggregation, so that they do not see the full extent of the aggregated proteins until ~55°C, at which point there is a sudden drop in amplitude; in the second measurement, where the entire CD spectrum is acquired, aggregation proceeds to completion prior to the time required to complete the scans, and they are monitoring only the CD from the monomers, as we do.

Unfolding with urea denaturation. It is important to compare our results on urea denaturation with those obtained by Kuramitsu and co-workers on *T. thermophilus* MutM protein (12). For *E. coli* Fpg, we find that the unfolding transition, as monitored by the shift in Trp fluorescence, exhibits a perfect two-state unfolding transition, and that the fraction of unfolded molecules thus obtained correlates beautifully with the loss in Fapy DNA glycosylase activity (Fig. 6). Kuramitsu and co-workers monitored the change in ellipticity at 222 nm with increasing urea concentration for *T. thermophilus* MutM and found that the unfolding transition involves a distinct intermediate. They have interpreted their results as indicative of a two-domain protein, with the two domains having a stability of 8.6 kcal/mol and 16.2 kcal/mol, respectively (12). X-ray crystal structure has since confirmed the existence of two domains for *T. Thermophilus* MutM (11). It is important to note that this difference in the unfolding behavior of the two proteins does not imply that they are structurally very different or that *E. coli* Fpg is a single-domain protein. In our measurements, we monitored the changes in tertiary structure with increasing urea, as probed by Trp fluorescence. In order to make a direct comparison of the unfolding behavior of the two proteins, it will be important to make CD and Trp fluorescence measurements with increasing urea for both proteins, as well as corresponding measurements of the loss of activity of *T. thermophilus* MutM protein.

A kinetic scheme for aggregation. The salient features of the observed kinetics of heat aggregation suggest the model

$$M + A_n \underset{k_2}{\overset{k_1}{\Longleftrightarrow}} (M \cdots A_n) \underset{k_4}{\overset{k_3}{\Longleftrightarrow}} A_{n+1}, \qquad [2]$$

where M denotes Fpg monomers (native or partially denatured); A_n and A_{n+1} are aggregates formed by n and $n + 1$ protein monomers, respectively, and $(M \cdots A_n)$ is the monomer-aggregate complex. The amplitude of the fluorescence signal, measured at one wavelength, monitors primarily the fractional population of monomers as a function of time, and cannot distinguish between native and partially denatured proteins. Therefore, partially denatured monomers are not explicitly included in the model. The complex is formed with a diffusion-limited rate constant k_1 and dissociates with a characteristic rate constant k_2. The aggregate grows and dissociates with the rate constants k_3 and k_4, respectively. If $k_2 \gg k_1$, the concentration of $(M \cdots A_n)$ complex is small at all times and we can assume the steady state approximation. The observed relaxation rate (k_{obs}) and the overall equilibrium constant (K) can then be written as (19)

$$k_{obs} = \frac{k_1 k_3 + k_2 k_4}{k_2 + k_3} \qquad [3]$$

$$K = \frac{k_1 k_3}{k_2 k_4} = \frac{[M]_0 - [M]_\infty}{[M]_\infty}, \qquad [4]$$

where $[M]_0$ is the initial concentration of the Fpg monomers and $[M]_\infty$ is the equilibrium concentration of the monomers (at the end of the heat aggregation process). From Eqs. [3] and [4] it follows that

$$k_{obs} = \frac{k_1 k_3}{k_2 + k_3}\left(\frac{[M]_0}{[M]_0 - [M]_\infty}\right). \qquad [5]$$

The ratio $([M]_0 - [M]_\infty)/[M]_0$ in Eq. [5] is the fraction of monomers that aggregate during the heat aggregation process and are obtained directly from the kinetics

measurements as the fractional amplitude of the fast component in the biexponential fit to the data.

In the scheme shown in Eq. [2], k_1 is assumed to be a pseudo-first order rate constant $k_1 = k_D[M]_0$, where k_D is the diffusion-limited bimolecular rate constant. We can write $k_D = 4\pi Dd10^3 N_A$ (in M^{-1} s^{-1}), where D is the sum of the diffusion coefficients of the monomer and the monomer-aggregate complex, d is some critical distance between the monomers and the complex, and N_A is Avogadro's number (20). In the initial stages of the aggregation process, we can approximate $k_D \approx (8RT/3\eta)10^3$ where η is the viscosity of the medium at temperature T; here we have used the Stoke–Einstein relation and assumed that d is approximately twice the radius a of the monomers. Thus, $k_1 \approx (8RT/3\eta)$ $10^3[M]_0 \approx 0.22\ T/\eta\ s^{-1}$ where T is in K, η is in kg m^{-1} s^{-1}, and we have used the initial concentration of protein monomers $[M]_0 = 10\ \mu M$. Similarly, the unimolecular rate constant k_2 that characterizes the dissociation of the monomer–aggregate complex is estimated as $k_2 = 4\pi Dd/\Delta V$ where ΔV is the volume of the monomer–aggregate complex and is approximately $4/3\pi d^3$ in the initial stages of the aggregation (20). Therefore, $k_2 \approx 3D/d^2 \approx RT/4\pi\eta a^3 N_A$ where we have used the same assumptions as for k_1. Using a value of $a \approx 2.1$ nm as the size of a monomer of Fpg (11), we obtain $k_2 \approx 118.6\ T/\eta\ s^{-1}$.

As the aggregation proceeds, the concentration of monomers depletes, the size of the complex increases, and the pseudo-first order approximation is no longer valid. The aggregation kinetics should deviate from a single-exponential. Our kinetics data are not sensitive to this deviation and are reasonably well described by a single-exponential phase during heat aggregation, presumably because the fraction of molecules that aggregate are less than 50% up to ~50°C.

To calculate the observed relaxation rate k_{obs} (defined in Eq. [5]) as a function of temperature we assume that k_3 has an Arrhenius temperature-dependence $k_3 = k_{30}\exp[-\Delta H/R(1/T - 1/T_0)]$, where $T_0 = 25$°C is chosen as a reference temperature, k_{30} is the rate constant for the step $(M \cdots A_n) \rightarrow A_{n+1}$ at $T = T_0$, and ΔH is the activation enthalpy for that step. The calculated values of k_{obs} were fitted to the measured relaxation rates corresponding to the fast component of the biexponential aggregation kinetics (Fig. 4b) with k_{30} and ΔH chosen as free parameters. The best fit values of the unknown parameters are $k_{30} = 9.3 \times 10^{-2}$ s^{-1}, and $\Delta H = 23$ kcal mol^{-1}. The value of the activation enthalpy for the step $(M \cdots A_n) \rightarrow A_{n+1}$ is very close to the value of the apparent activation energy $E_a = 21$ kcal mol^{-1} calculated directly from an Arrhenius fit to the observed rates shown in Fig. 4b. These results show that the rate-limiting step for the heat aggregation is the reaction step $(M \cdots A_n) \rightarrow A_{n+1}$ which corresponds to the addition of a monomer to the aggregate.

Urea dependence of the aggregation kinetics. Hydrophobic interactions are known to play a crucial role in aggregation processes (21, 22). Our results show that heat aggregation of Fpg results from conformational changes of Fpg tertiary structure by increasing the exposure of apolar patches at the protein surface with increasing temperature, leading to an increase in the hydrophobic interaction between partially unfolded proteins to form aggregates. If Fpg aggregates have a hydrophobic nature then the aggregation process can be altered by chemical denaturant which reduces hydrophobic interactions between monomers in protein aggregate and increases the solubility of aggregates. At high concentration of urea the increase of solubility of the aggregates is expected to be the dominating factor (21) leading to a decrease in propensity to aggregate. Indeed, Fig. 7 shows that the amplitude of the heat aggregation drops sharply above ~3 M urea concentration. In the context of our model, increased concentration of urea is expected to decrease k_3 and increase k_4, thus decreasing the overall equilibrium constant K for forming aggregates.

SUMMARY AND CONCLUSIONS

Using CD, scattered light, and Trp fluorescence measurements, we show that the *E. coli* Fpg protein irreversibly aggregates under heating at temperatures above 35°C, i.e., at physiological temperatures. The kinetics of aggregation show an Arrhenius temperature-dependence with an apparent activation enthalpy of ~21 kcal/mol. The heat aggregation is preceded by changes in tertiary structure of the Fpg monomers. The secondary structure of the fraction that does not aggregate remains unchanged. We have presented a simple kinetic scheme, consistent with the aggregation kinetics observed for *E. coli* Fpg, and which suggests that the rate-limiting step, and which is also the highly activated step, is the addition (and dissociation) of a monomer to (and from) the aggregate-complex. We find that the stability of the *E. coli* Fpg protein is 3.6 kcal/mol which is about 3 times less than for *T. thermophilus* MutM protein. The relative instability of the *E. coli* Fpg makes this protein more susceptible to aggregation by increasing the exposure of apolar patches at the protein surface with increasing the temperature, leading to an increased propensity for intermolecular hydrophobic interactions between partially unfolded proteins to form aggregates. In support of this hypothesis, we find that both addition of glycerol and an increase in urea concentration, inhibit aggregation. Addition of glycerol increases the stability of the protein, thus inhibiting the conformational changes that precede aggregation. Increase in the urea concentration reduces intermolecular hydrophobic interactions and destabilizes the monomer-aggregate complex, with essentially no aggregation observed above ~3 M urea.

ACKNOWLEDGMENTS

We are greatly indebted to Professor Timothy A. Keiderling for his support with CD measurements. We thank Dr. J.-C. Brochon for helpful comments on the manuscript and Dr. S. V. Provencher for kindly providing us with a CONTIN program and its description. This work was supported in part by National Science Foundation and by the donors of the Petroleum Research Fund, administered by the American Chemical Society.

REFERENCES

1. Tchou, J., Kasai, H., Shibutani, S., Chung, M. H., Laval, J., Grollman, A. P., and Nishimura, S. (1991) 8-Oxoguanine (8-hydroxyguanine) DNA glycosylase and its substrate specificity. *Proc. Natl. Acad. Sci. USA* **88,** 4690–4694.
2. Lindahl, T. (1993) Instability and decay of the primary structure of DNA. *Nature* **362,** 709–715.
3. Cleaver, J. E., and Kraemer, K. H. (1989) The Metabolic Basis of Inherited Disease, McGraw-Hill, New York.
4. Laval, J., Jurado, J., Saparbaev, M., and Sidorkina, O. (1998) Antimutagenic role of base-excision repair enzymes upon free radical-induced DNA damage. *Mutat. Res.* **402,** 93–102.
5. Tchou, J., and Grollman, A. P. (1995) The catalytic mechanism of Fpg protein. Evidence for a Schiff base intermediate and amino terminus localization of the catalytic site. *J. Biol. Chem.* **270,** 11671–11677.
6. Michaels, M. L., Cruz, C., Grollman, A. P., and Miller, J. H. (1992) Evidence that MutY and MutM combine to prevent mutations by an oxidatively damaged form of guanine in DNA. *Proc. Natl. Acad. Sci. USA* **89,** 7022–7025.
7. Boiteux, S. (1993) Properties and biological functions of the NTH and FPG proteins of *Escherichia coli:* Two DNA glycosylases that repair oxidative damage in DNA. *J. Photochem. Photobiol.: B* **19,** 87–96.
8. O'Conor, T. R., and Laval, J. (1989) Physical association of the 2,6-diamino-4-hydroxy 5-*N*-formamidopyrimidine–DNA glycosylase of *Escherichia coli* and an activity nicking DNA at apurinic/apyrimidinic sites. *Proc. Natl. Acad. Sci. USA* **86,** 5222–5226.
9. Bailly, V., Verly, W. G., O'Connor, T., and Laval, J. (1989) Mechanism of DNA strand nicking at apurinic/apyrimidinic sites by *Escherichia coli* [formamidopyrimidine] DNA glycosylase. *Biochem. J.* **262,** 581–589.
10. Graves, R. J., Felzenszwalb, I., Laval, J., and O'Connor, T. R. (1992) Excision of 5′-terminal deoxyribose phosphate from damaged DNA is catalyzed by the Fpg protein of *Escherichia coli*. *J. Biol. Chem.* **267,** 14429–14435.
11. Sugahara, M., Mikawa, T., Kumasaka, T., Yamamoto, M., Kato, R., Fukuyama, K., Inoue, Y., and Kuramitsu, S. (2000) Crystal structure of a repair enzyme of oxidatively damaged DNA, MutM (Fpg), from an extreme thermophile, *Thermus thermophilus* HB8. *EMBO J.* **19,** 3857–3869.
12. Mikawa, T., Kato, R., Sugahara, M., and Kuramitsu, S. (1998) Thermostable repair enzyme for oxidative DNA damage from extremely thermophilic bacterium, *Thermus thermophilus* HB8. *Nucleic Acids Res.* **26,** 903–910.
13. Buchko, G. W., Hess, N. J., Bandaru, V., Wallace, S. S., and Kennedy, M. A. (2000) Spectroscopic studies of zinc(II)- and cobalt(II)-associated *Escherichia coli* formamidopyrimidine-DNA glycosylase: Extended X-ray absorption fine structure evidence for a metal-binding domain. *Biochemistry* **39,** 12441–12449.
14. Boiteux, S., O'Connor, T. R., and Laval, J. (1987) Formamidopyrimidine-DNA glycosylase of *Escherichia coli:* Cloning and sequencing of the *fpg* structural gene and overproduction of the protein. *EMBO J.* **10,** 3177–3183.
15. Pace, C. N. (1986) Determination and analysis of urea and guanidine hydrochloride denaturation curves. *Methods Enzymol.* **131,** 266–280.
16. Sousa, R. (1995) Use of glycerol and other protein structure stabilizing agents in protein crystallization. *Acta Crystallogr.* **D51,** 271–277.
17. Sidorkina, O. M., Kuznetsov, S. V., Blais, J. C., Bazin, M., Laval, J., and Santus, R. (1999) Ultraviolet-B-induced damage to *Escherichia coli* Fpg protein. *Photochem. Photobiol.* **69,** 658–663.
18. Provencher, S. W., and Glockner, J. (1981) Estimation of globular protein secondary structure from circular dichroism. *Biochemistry* **20,** 33–37.
19. Wang, J. C., and Davidson, N. (1966) Thermodynamic and kinetic studies on the interconversion between the linear and circular forms of phage lambda DNA. *J. Mol. Biol.* **15,** 111–123.
20. Steinfeld, J. I., Francisco, J. S., and Haas, W. L. (1999) Chemical Kinetics and Dynamics, Prentice Hall, New Jersey.
21. De Young, L. R., Dill, K. A., and Fink, A. L. (1993) Aggregation and denaturation of apomyoglobin in aqueous urea solutions. *Biochemistry* **32,** 3877–3886.
22. Hummer, G., Garde, S., Garcia, A. E., Paulaitis, M. E., and Pratt, L. R. (1998) The pressure dependence of hydrophobic interactions is consistent with the observed pressure denaturation of proteins. *Proc. Natl. Acad. Sci. USA* **95,** 1552–1555.